

PMSM Sensorless Control System Based on DTC Using FLC and Luenberger-PLL Observer

Claudiu-Ionel Nicola

Research Department

National Institute for Research, Development and Testing in Electrical Engineering – ICMET Craiova
Department of Automatic Control and Electronics
University of Craiova
Craiova, Romania
nicolaclaudiu@icmet.ro, claudiu.nicola@edu.ucv.ro

Marcel Nicola

Research Department

National Institute for Research, Development and Testing in Electrical Engineering – ICMET Craiova
Department of Automatic Control and Electronics
University of Craiova
Craiova, Romania
marcel_nicola@icmet.ro, marcel.nicola@edu.ucv.ro

Andreea Iacob

Department of Automatic Control and Electronics
University of Craiova
Craiova, Romania
andreea.iacob@edu.ucv.ro

Cristian Pîrvu

Department of Automatic Control and Electronics
University of Craiova
Craiova, Romania
cristian.pirvu@edu.ucv.ro

Abstract—Starting from the desire to achieve a good control performance of the Permanent Magnet Synchronous Motor (PMSM), but with a relatively medium complexity of the control system, this paper presents a sensorless control structure of a PMSM using the Direct Torque Control (DTC) control strategy. In order to improve the performance of the Luenberger observer used for speed estimation, a Phase Locked Loop (PLL) observer is additionally used which, due to the integral nature of the control system, ensures a better estimation of the PMSM rotor speed. In addition, the classic PI controller used for speed control is continuously adjusted by a Fuzzy Logic Controller (FLC). In contrast to the usual case where the input to the fuzzy controller is given by the speed error and its derivative, this paper proposes a second fuzzy controller which additionally uses an input provided by a load torque observer. The superior performance of the proposed PMSM sensorless control system is demonstrated by numerical simulations in both stationary and dynamic modes.

Keywords—PMSM, DTC, Fuzzy Logic Control, Luenberger Observer, Phase Locked Loop Observer.

I. INTRODUCTION

The advantages of using PMSM in precision electric actuators have been the basis for the development of various control systems, ranging from those based on PI controllers [1, 2] to adaptive [3, 4], predictive [5, 6], robust [7, 8], fuzzy [9-11], and neuronal [12, 13] type controllers.

Typical control strategies for PMSM are Field Oriented Control (FOC) [14, 15] and DTC [16-18]. The attempt to obtain a high performance of the PMSM control system, both in static and dynamic mode, where the load torque has relatively large variations, can be done with the help of controllers that are clearly superior to the classical PI type controllers, which are able to ensure a good performance only

This paper was elaborated as part of the NUCLEU Program within the framework of the National Research, Development, and Innovation Plan for 2022-2027, developed with the support of the Ministry of Research, Innovation, and Digitization, Project No. PN 23 33 02 04 and Installation of National Interest “System for generating, measuring and recording short circuit currents” - SPMICS.

in certain parts of the operating range of the parameters and the evolution of the load torque. In order to keep a relatively optimal ratio between the performance of the controller given the possibility of real-time implementation and its cost, it is proposed to keep a PI type controller, but whose tuning parameters are adapted by a fuzzy logic system.

Therefore, in this paper, in the case of keeping the PI type primary controller for speed control and using ON-OFF type hysteresis controllers for torque and flux control, it is proposed to use two fuzzy type controllers in order to obtain a good performance of the PMSM control system, both in static and dynamic regime under the conditions of relatively high load torque variation. Furthermore, in order to obtain the sensorless character of the PMSM control system based on the DTC strategy, a classical Luenberger observer [19-20] is used, to which a PLL observer [21-22] is added, which, due to its integrative character, provides a superior estimation of the PMSM rotor speed.

The rest of the paper is structured as follows: Sec. II presents the proposed architecture of the PMSM sensorless control system based on the DTC strategy, while the implementation of the FLC-type controller used to adjust the tuning PI parameters is shown in Sec. III. Section IV shows the numerical simulations performed in the Matlab/Simulink programming environment for the proposed PMSM sensorless control system, and the last section presents some conclusions and some directions for future work.

II. PMSM SENSORLESS CONTROL SYSTEM BASED ON DTC

The usual equations of operation of a PMSM in the d - q reference frame solidar with the rotor are as follows [15, 16]:

$$\begin{bmatrix} \lambda_d \\ \lambda_q \end{bmatrix} = \begin{bmatrix} L_d & 0 \\ 0 & L_q \end{bmatrix} \begin{bmatrix} i_d \\ i_q \end{bmatrix} + \begin{bmatrix} \lambda_0 \\ 0 \end{bmatrix} \quad (1)$$

$$\begin{bmatrix} u_d \\ u_q \end{bmatrix} = R_s \begin{bmatrix} i_d \\ i_q \end{bmatrix} + \begin{bmatrix} L_d & 0 \\ 0 & L_q \end{bmatrix} \frac{d}{dt} \begin{bmatrix} i_d \\ i_q \end{bmatrix} + n_p \omega \begin{bmatrix} 0 & -L_d \\ L_d & 0 \end{bmatrix} \begin{bmatrix} i_d \\ i_q \end{bmatrix} + n_p \omega \begin{bmatrix} 0 \\ \lambda_0 \end{bmatrix} \quad (2)$$

$$T_e = \frac{3}{2} n_p ((L_d - L_q) i_d i_q + \lambda_0 I_q) \quad (3)$$

$$J \dot{\omega} = T_e - T_L - B \omega \quad (4)$$

The notations are the usual ones for stator resistance and inductance on the d - q axes, while the mechanical quantities ω and θ represent the speed and angle of the PMSM rotor respectively. It can be noted that the electrical quantities ω_e it is defined like $\omega_e = n_p \omega$. Fluxes on the d and q axes are denoted by λ_d , λ_q and λ_0 is the flux coupling. In addition, n_p is the number of pole pairs, B is the viscous friction coefficient, J and T_L are the PMSM rotor inertia and load torque respectively. To simplify, the following equalities are assumed to be true: $L_d = L_q$ and $R_d = R_q = R_s$ [18]. Figure 1 shows the general architecture proposed for the control of a DTC-based PMSM. Flux and torque are usually estimated by a specialised observer [16]. Speed can be measured directly or estimated in sensorless control. In this case, it is proposed to use a Luenberger observer working in conjunction with a PLL. PMSM control is implemented in a cascade control structure where the outer speed control loop is controlled by a PI controller in conjunction with a fuzzy controller. Inner torque and flux control loop contains ON-OFF hysteresis controllers.

In the abc three-phase frame, the PMSM equations are as follows:

$$\begin{cases} u_a = i_a R_s + \frac{d\lambda_a}{dt} \\ u_b = i_b R_s + \frac{d\lambda_b}{dt} \\ u_c = i_c R_s + \frac{d\lambda_c}{dt} \end{cases} \quad (5)$$

where: λ_a , λ_b , and λ_c are the three-phase flux linkage corresponding on abc frame stator winding and are given by the following relationship:

$$\begin{cases} \lambda_a = i_a L + \lambda_0 \\ \lambda_b = i_b L + \lambda_0 \\ \lambda_c = i_c L + \lambda_0 \end{cases} \quad (6)$$

For the description of the PMSM rotor speed observer equations, the representation in the α - β reference frame solid with the stator is used:

$$\begin{cases} L \frac{di_\alpha}{dt} = u_\alpha - e_\alpha - R_s i_\alpha \\ L \frac{di_\beta}{dt} = u_\beta - e_\beta - R_s i_\beta \end{cases} \quad (7)$$

where: e_α and e_β represents the back-EMF of PMSM. These can be expressed as the relationship (8) [16].

$$\begin{cases} e_\alpha = -\lambda_0 \omega_e \sin \theta_e \\ e_\beta = \lambda_0 \omega_e \cos \theta_e \end{cases} \quad (8)$$

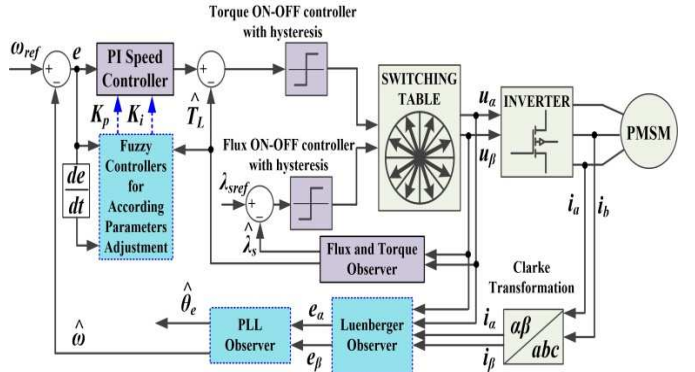


Fig. 1. General structure of the proposed PMSM sensorless control system for PMSM based on DTC strategy.

Figure 2 shows the general scheme of a Luenberger observer, where the notations are the usual ones for currents and voltages in the α - β reference frame. The convention is that a quantity to which the symbol $\hat{\cdot}$ is added is an estimate of that quantity.

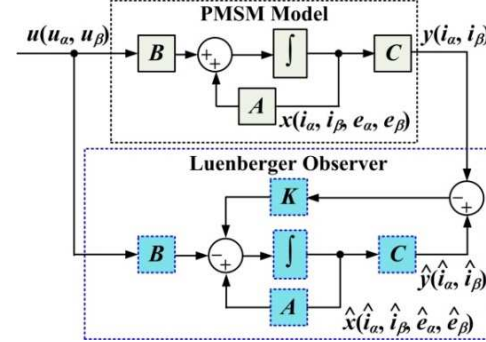


Fig. 2. Block diagram of the Luenberger observer.

For a system of the type described in relation (9), the Luenberger observer is associated in relation (10), whose particularisation for the presented system is given in relation (11) [18, 19].

$$\begin{cases} \dot{x} = Ax + Bu \\ y = Cx \end{cases} \quad (9)$$

$$\begin{cases} \dot{\hat{x}} = A\hat{x} + Bu - K(y - \hat{y}) \\ \hat{y} = C\hat{x} \end{cases} \quad (10)$$

$$\begin{cases} L \frac{d\hat{i}_\alpha}{dt} = u_\alpha - \hat{e}_\alpha - R_i \alpha + K_{LO1}(i_\alpha - \hat{i}_\alpha) \\ L \frac{d\hat{i}_\beta}{dt} = u_\beta - \hat{e}_\beta - R_i \beta + K_{LO1}(i_\beta - \hat{i}_\beta) \end{cases} \quad (11)$$

where:

$$\begin{cases} \hat{\dot{e}}_\alpha = -K_{LO1}(i_\alpha - \hat{i}_\alpha) \\ \hat{\dot{e}}_\beta = -K_{LO2}(i_\beta - \hat{i}_\beta) \end{cases} \quad (12)$$

where K_{LO1} and K_{LO2} are the Luenberger observer gains.

Using the estimates of the back EMF defined in relation (8) in relation (12), it is possible to calculate the electrical angle and speed of the PMSM rotor as in relation (13).

$$\begin{cases} \hat{\theta}_e = \arctan \left(-\frac{\hat{\dot{e}}_\alpha}{\hat{\dot{e}}_\beta} \right) \\ \hat{\omega}_e(t) = \frac{\sqrt{\hat{\dot{e}}_\alpha^2 + \hat{\dot{e}}_\beta^2}}{\lambda_0} \end{cases} \quad (13)$$

According to [16], a series of appropriately designed filters are used to reduce the oscillations and imprecision of the numerical implementation of relation (13). According to [18], an alternative is to use a PLL loop containing a PI controller, which naturally filters the output signal representing the speed estimate. In this way, according to the PLL block diagram shown in Figure 3, the relationship (14) can be obtained.

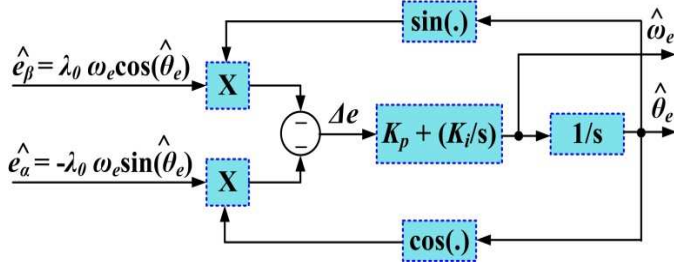


Fig. 3. Block diagram of the PLL observer.

$$\begin{aligned} \Delta e &= -\hat{\dot{e}}_\alpha \cos(\hat{\theta}) - \hat{\dot{e}}_\beta \sin(\hat{\theta}) = \\ &= \lambda_0 \hat{\omega}_e \sin(\hat{\theta}_e - \hat{\theta}) \end{aligned} \quad (14)$$

Next, for small values of the estimation error of the PMSM rotor electrical angle, the approximation in relation (15) is obtained:

$$\sin(\hat{\theta}_e - \hat{\theta}) \approx \hat{\theta}_e - \hat{\theta} \quad (15)$$

The block diagram in Figure 3 can thus be reconstructed in the form shown in Figure 4, which shows that the PMSM rotor speed estimate is obtained.

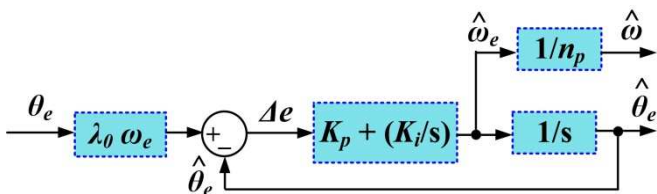


Fig. 4. Equivalent block diagram of the PLL observer.

III. FUZZY LOGIC CONTROL OF PMSM

As shown in Figure 1, the speed controller is a PI controller whose tuning parameters K_p and K_i are continuously adjusted by a fuzzy controller whose weighted outputs represent the adjustments of parameters K_p and K_i . In the proposed approach, two fuzzy controllers are actually used, the main one that adjusts the K_p and K_i parameters according to the speed error and its derivative, and a second one that helps to adjust the K_p and K_i parameters according to the evolution of the load torque. This results in superior control system performance in both static and dynamic modes. The second fuzzy controller is used to obtain good dynamic performance in a specific case, when the speed step is decreasing and the load torque is relatively high. As presented in [8], the PI controller or the combined use of the main fuzzy controller alone cannot suppress the negative override that occurs in this case. Thus, Table I shows the rules of the main fuzzy controller implemented in Matlab Fuzzy Logic Toolbox [23]. The linguistic quantities SE (speed error) and SED (speed error derivative) are represented linguistically as {NB - negative big, NS - negative small, ZO - zero, PS - positive small, PB - positive big}. The values of E and DE are normalised in the range [-1, 1]. For the output quantities K_pF , K_iF , the linguistic values are {Z - zero, S - small, M - medium, B - big}. Note that the implementation in Matlab Fuzzy Logic Toolbox (see Figure 5) uses the Mamdani inference method and the centroid method for defuzzification.

TABLE I. FUZZY LOGIC RULES FOR PI SPEED CONTROLLER TUNING PARAMETERS K_pF AND K_iF

K_pF	K_iF	SE				
		NB	NS	ZO	PS	PB
SED	NB	B	Z	M	M	B
	NS	B	Z	B	M	B
	ZO	B	Z	S	M	Z
	PS	B	Z	S	M	S
	PB	M	Z	S	M	B

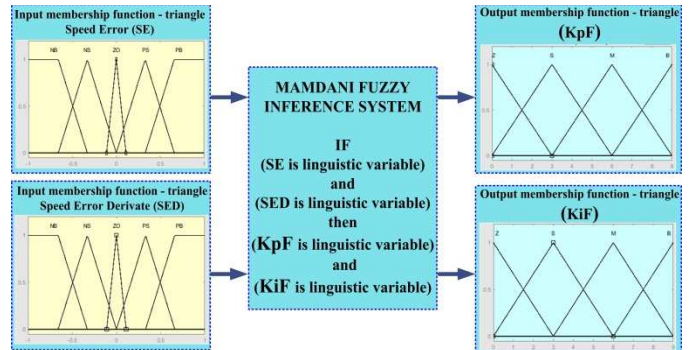


Fig. 5. Fuzzy logic controller for adjusting PI speed controller tuning parameters K_p and K_i .

The implementation of the fuzzy controller in the Fuzzy Logic Toolbox, which additionally adjusts the parameters K_p and K_i according to the load torque variation, but also the SE and SED values, is shown in Figure 6. The linguistic values for SE and SED are different from those defined in the first fuzzy controller, being structured in fewer intervals to emphasise a greater weighting of the load torque variation. For SE and SED, the linguistic representation is as follows: {N - negative, Z - zero, P - positive}.

For TLF, the linguistic representation is as follows {L - low, M - medium, H - high}. For the output KpF&KiF, the linguistic values are as follows {VL - very low, L - low, M - medium, H - high}.

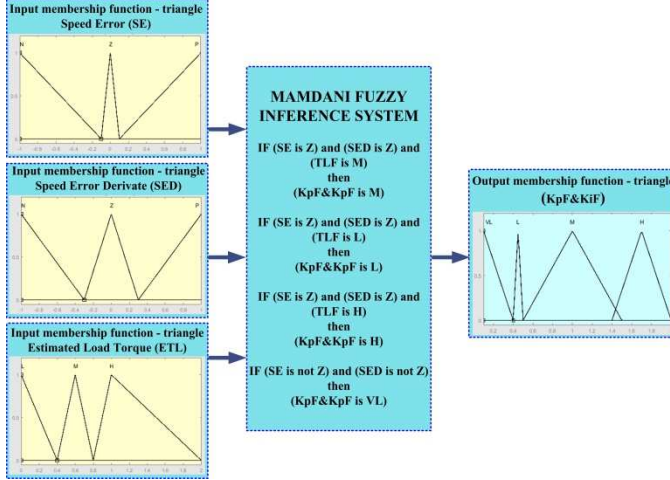


Fig. 6. Fuzzy logic controller improvement for adjusting the tuning of the PI speed controller parameters K_p and K_i .

IV. NUMERICAL SIMULATIONS

The block diagram of the Matlab/Simulink model implementation for the PMSM sensorless control system based on the DTC strategy using FLC to adjust the PI tuning parameters using the Luenberger-PLL observer is shown in Figure 7. The numerical simulations performed are based on the nominal PMSM parameters given in Table II. The implementation of the Simulink model of the proposed control

system is based on Figure 1. The simulation time is 0.00001s. Also, the parameters of the Luenberger observer are $K_{LO1} = 201$ and $K_{LO2} = 1.05$. The PI controller parameters of the PLL observer structure are $K_{pPLL} = 150$ and $K_{iPLL} = 2000$.

TABLE II. PMSM PARAMETER VALUES

IPMSM parameter	Value	Unit
R_s	2.875	Ω
L_d	0.0085	H
L_q	0.0085	H
J	0.008	$\text{kg}\cdot\text{m}^2$
B	0.005	$\text{N}\cdot\text{m}\cdot\text{s}/\text{rad}$
λ_0	0.175	Wb
n_p	4	—

For a PMSM rotor reference speed evolution sequence of the form: $\omega_{ref} = [100 \ 600 \ 900]\text{rpm} \rightarrow [0 \ 0.1 \ 0.2]\text{s}$ and a load torque evolution sequence $T_L = [0.1 \ 1 \ 1.5]\text{Nm} \rightarrow [0 \ 0.1 \ 0.2]\text{s}$, the numerical simulations show the evolution of the sensorless PMSM control system based on the DTC strategy and the use of the two Luenberger and Luenberger-PLL observers for speed estimation presented in Section II.

Thus, Figures 8 and 9 show the evolution of the sensorless PMSM control system when using the two types of observers. The comparison of the evolution of the estimated speeds is shown in Figure 10. In the detail of the figure, it can be seen that the settling time for the Luenberger observer is 12.3ms and for the Luenberger-PLL observer the settling time is 10.9ms. Another indicator of the performance of the PMSM sensorless control system is the estimated speed signal ripple, which has a value of 40.61rpm when using the Luenberger observer and 38.32rpm when using the Luenberger-PLL observer.

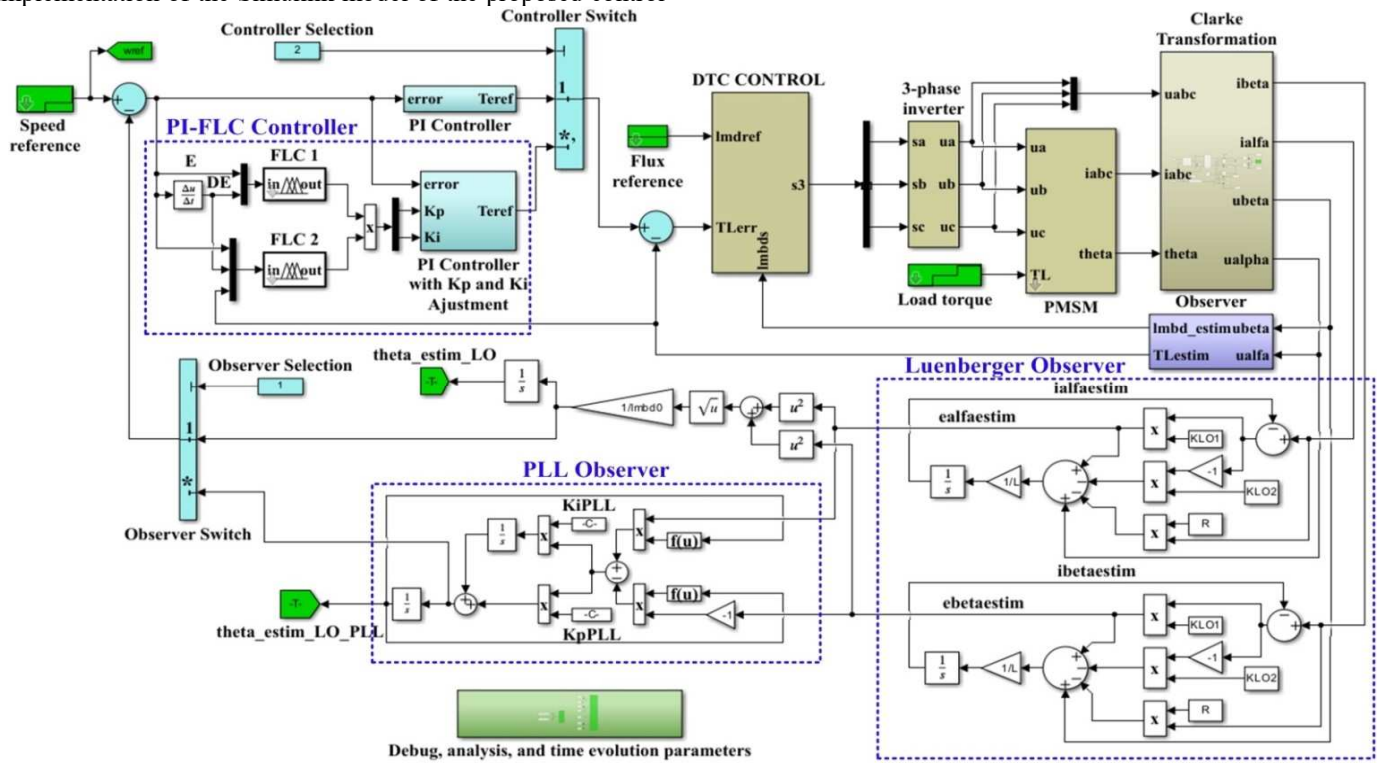


Fig. 7. Matlab/Simulink implementation for PMSM sensorless control system based on the DTC strategy using FLC to adjust the PI tuning parameters using the Luenberger-PLL observer.

In the following simulations, speed estimation is performed using a Luenberger-PLL observer. The evolution of the PMSM control system in terms of its performance using the PI type speed controller and the FLC type speed controller adjusting the controller tuning parameters in Figures 11 and 12 shows the evolution of the PMSM parameters concerned.

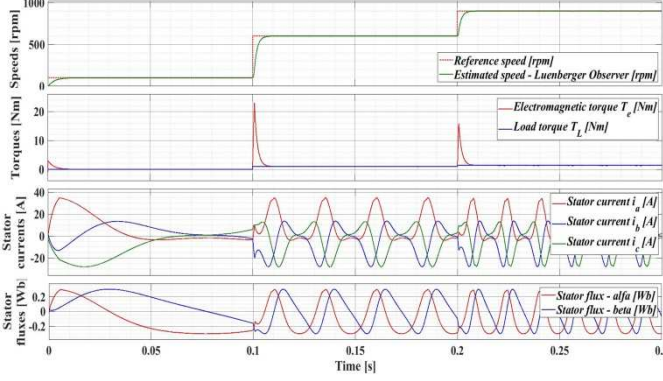


Fig. 8. Numerical simulation and parameter evolution of PMSM sensorless control system based on DTC strategy using Luenberger observer.

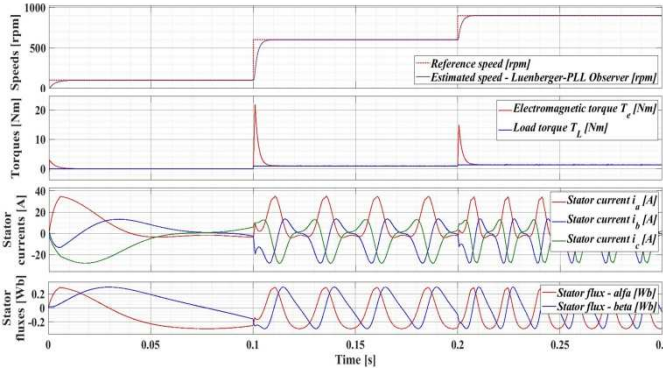


Fig. 9. Numerical simulation and parameter evolution of PMSM sensorless control system based on DTC strategy using Luenberger-PLL observer.

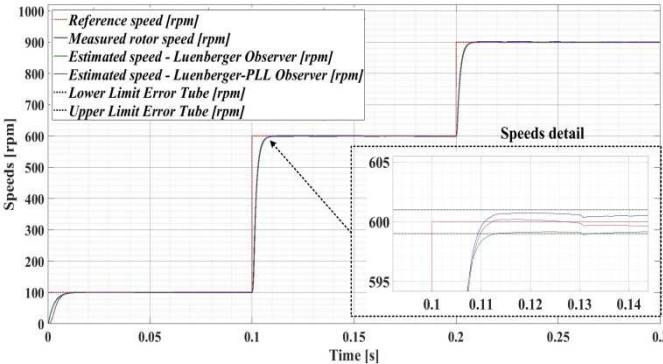


Fig. 10. Comparison of estimated speed evolution for PMSM sensorless control based on DTC strategy using Luenberger observer and Luenberger-PLL observer.

In addition, the speed comparison is carried out for a PMSM rotor reference speed evolution sequence of the following form: $\omega_{ref} = [100 \ 300 \ 600 \ 900 \ 500 \ 300] \text{ rpm} \rightarrow [0.05 \ 0.1 \ 0.15 \ 0.2 \ 0.25] \text{ s}$ and a sequence of load torque evolution, respectively $T_L = [0.1 \ 1 \ 1.5 \ 0.5 \ 1.5 \ 1] \text{ Nm} \rightarrow [0 \ 0.05 \ 0.1 \ 0.15 \ 0.2 \ 0.25] \text{ s}$.

In the detail of Figure 13, it can be seen that the settling time is 9.9ms when using the classical PI controller, and 3.2ms when using the FLC controller, which adjusts the tuning parameters of the PI controller.

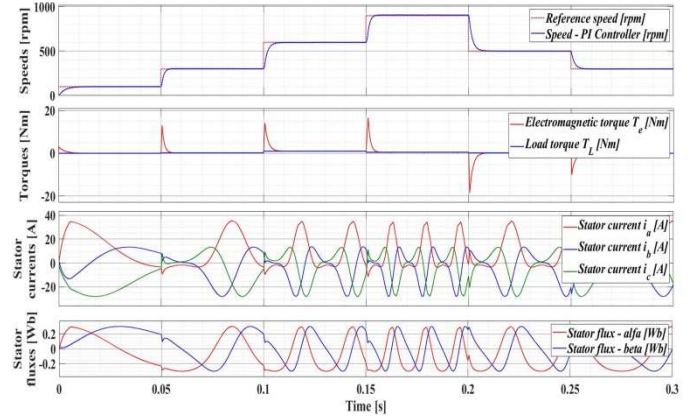


Fig. 11. Numerical simulation and parameter evolution of PMSM sensorless control system based on DTC strategy using PI speed controller.

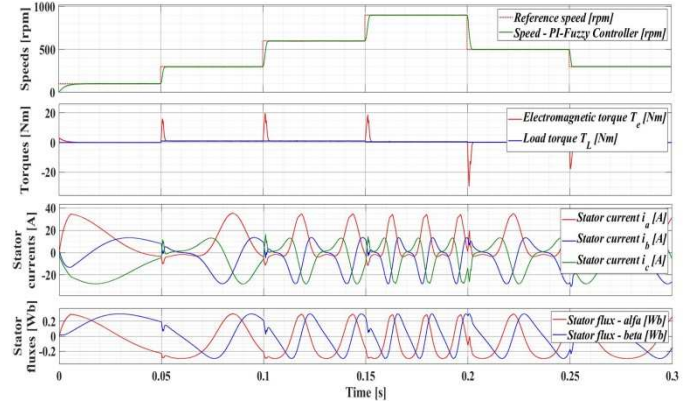


Fig. 12. Numerical simulation and parameter evolution of the PMSM sensorless control system based on DTC strategy using FLC for PI speed controller tuning parameter adjustment.

Furthermore, the performance of the control system for the two types of speed controllers used is analysed in terms of speed signal ripple, and the values of this performance indicator are 37.56rpm for the PI speed controller and 33.72rpm for the FLC-based PI speed controller.

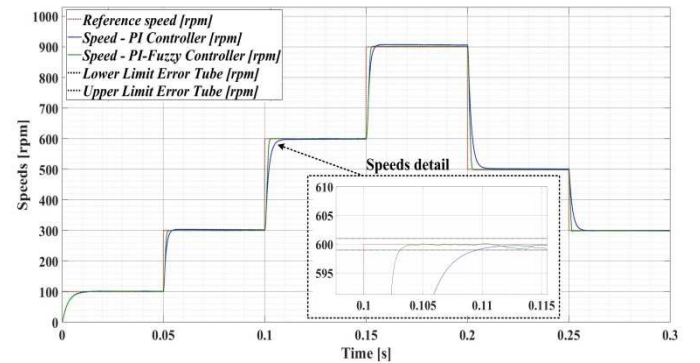


Fig. 13. Comparison of speed evolution for PMSM sensorless control based on DTC strategy using PI speed controller and FLC for PI speed controller tuning parameter adjustment.

V. CONCLUSIONS

This paper presents a sensorless control structure of a PMSM using the DTC control strategy. The usual Luenberger-type observer used for speed estimation is improved by adding a PLL-type observer to obtain a better estimate of the PMSM rotor speed. In addition, the classic PI controller used for speed control is continuously adjusted by a fuzzy controller. In contrast to the usual case where the input to the fuzzy controller is given by the speed error and its derivative, in this paper a second fuzzy controller is implemented which additionally uses an input provided by a load torque observer to achieve a better performance of the control system.

The proposed fuzzy controller structures and their implementation in Matlab Fuzzy Logic Toolbox along with the Luenberger-PLL observer structure and numerical simulations of the proposed sensorless control system are also presented. Its superior performance is demonstrated in contrast to the usual related approaches. Future work will analyse fuzzy control structures improved by optimising the rules used and implementation in real time using a low/medium cost of embedded system.

REFERENCES

- [1] R. Harikrishnan and A. E. George, "Direct Torque Control of PMSM using hysteresis modulation, PWM and DTC PWM based on PI Control for EV - A comparative analysis between the three strategies," *The 2nd International Conference on Intelligent Computing, Instrumentation and Control Technologies (ICICICT)*, Kannur, India, 2019, pp. 566-571.
- [2] T. Zwergler and P. Mercorelli, "Combining a PI Controller with an Adaptive Feedforward Control in PMSM," *The 21th International Carpathian Control Conference (ICCC)*, High Tatras, Slovakia, 2020, pp. 1-5.
- [3] B. Singh and M. Kashif, "PF-MRAC-Based Elimination of Sensors in Solar-Powered PMSM Drive-Based Water Pumping System," in *IEEE Transactions on Industrial Electronics*, vol. 70, no. 11, pp. 11390-11400, November 2023.
- [4] S. Kumar and B. Singh, "Modified Model Reference Adaptive Sensorless Control of PMSM Driven LEV with Online Self-Tuning Speed Controller," *IEEE International Conference on Power Electronics, Drives and Energy Systems (PEDES)*, Jaipur, India, 2022, pp. 1-6.
- [5] Y. Li, P. Zhang, J. Hang, S. Ding, L. Liu, Q. Wang, "Comparison of dynamic characteristics of field oriented control and model predictive control for permanent magnet synchronous motor," *The 13th IEEE Conference on Industrial Electronics and Applications (ICIEA)*, Wuhan, China, 2018, pp. 2431-2434.
- [6] G. Wu, S. Huang, Q. Wu, F. Rong, C. Zhang, W. Liao, "Robust Predictive Torque Control of N*3-Phase PMSM for High-Power Traction Application," in *IEEE Transactions on Power Electronics*, vol. 35, no. 10, pp. 10799-10809, October 2020.
- [7] H. Guo, J. Xu and Y. -H. Chen, "Robust Control of Fault-Tolerant Permanent-Magnet Synchronous Motor for Aerospace Application With Guaranteed Fault Switch Process," in *IEEE Transactions on Industrial Electronics*, vol. 62, no. 12, pp. 7309-7321, December 2015.
- [8] M. Nicola, C. -I. Nicola, M. Duță, "Adaptive Sensorless Control of PMSM using Back-EMF Sliding Mode Observer and Fuzzy Logic," *Electric Vehicles International Conference (EV)*, Bucharest, Romania, 2019, pp. 1-6.
- [9] R. Sancio, S. Pugliese, K. Debbadi, M. Liserre, E. Brescia, G. L. Cascella, "Fuzzy Based Adaptive Linear Active Disturbance Rejection Control for an High speed PMSM," *IEEE 1st Industrial Electronics Society Annual On-Line Conference (ONCON)*, kharagpur, India, 2022, pp. 1-6.
- [10] N. Lakshmipriya, S. Ayyappan, R. Prabu, M. Hariprabhu, "An Intelligent Hybrid Fuzzy PI controller for Performance Analysis of Permanent Magnet Synchronous Motor," *The 5th International Conference on Smart Systems and Inventive Technology (ICSSIT)*, Tirunelveli, India, 2023, pp. 350-356.
- [11] M. Nicola, C. -I. Nicola, M. Duță, "Sensorless Control of PMSM using FOC Strategy Based on Multiple ANN and Load Torque Observer," *International Conference on Development and Application Systems (DAS)*, Suceava, Romania, 2020, pp. 32-37.
- [12] T. Tarczewski, Ł. Niewiara, Ł. M. Grzesiak, "Torque ripple minimization for PMSM using voltage matching circuit and neural network based adaptive state feedback control," *The 16th European Conference on Power Electronics and Applications*, Lappeenranta, Finland, 2014, pp. 1-10.
- [13] C. -I. Nicola, M. Nicola, S. Popescu, M. Duță, "Power Factor Correction and Sensorless Control of PMSM Using FOC Strategy," *International Conference on Electromechanical and Energy Systems (SIELMEN)*, Craiova, Romania, 2019, pp. 1-6.
- [14] R. G. Iturra and P. Thiemann, "Sensorless Field Oriented Control of PMSM using Direct Flux Control with improved measurement sequence," *The 21 XVIII International Scientific Technical Conference Alternating Current Electric Drives (ACED)*, Ekaterinburg, Russia, 2021, pp. 1-6.
- [15] W. Wu, F. Xie, G. Li, K. Liang, C. Qiu, H. Jiang, "Research on Direct Torque Control Based on RZVSVPWM of PMSM," *The 14th IEEE Conference on Industrial Electronics and Applications (ICIEA)*, Xi'an, China, 2019, pp. 2507-2511.
- [16] M. Nicola and C. -I. Nicola, "Improvement Performances of Sensorless Control for PMSM Based on DTC Strategy Using SMO Observer and RL-TD3 Agent," *The 5th Global Power, Energy and Communication Conference (GPECOM)*, Nevşehir, Turkiye, 2023, pp. 131-136.
- [17] S. Kumar and J. Seshadrinath, "An Investigation on SMC-DTC Technique Using SVM for PMSM Drive," *IEEE 3rd International Conference on Sustainable Energy and Future Electric Transportation (SEFET)*, Bhubaneswar, India, 2023, pp. 1-6.
- [18] R. Luo, Z.i Wang, Y. Sun, "Optimized Luenberger Observer-Based PMSM Sensorless Control by PSO" in *Modelling and Simulation in Engineering*, vol. 2022, pp. 1-17, August 2022.
- [19] M. Nicola and C. -I. Nicola, "Improvement Performances of Sensorless Control for PMSM Based on FOC Strategy Using Luenberger Observer, Sine Cosine Algorithm, and RL-TD3 Agent," *International Conference on Electromechanical and Energy Systems (SIELMEN)*, Craiova, Romania, 2023, pp. 1-7.
- [20] C. Lascau and G. -D. Andreescu, "PLL Position and Speed Observer With Integrated Current Observer for Sensorless PMSM Drives," in *IEEE Transactions on Industrial Electronics*, vol. 67, no. 7, pp. 5990-5999, July 2020.
- [21] M. H. Bierhoff, "A General PLL-Type Algorithm for Speed Sensorless Control of Electrical Drives," in *IEEE Transactions on Industrial Electronics*, vol. 64, no. 12, pp. 9253-9260, December 2017.
- [22] Y. Ge, W. Song, Y. Yang, P. Wheeler, "A Polar-Coordinate-Multisignal-Flux-Observer-Based PMSM Non-PLL Sensorless Control," in *IEEE Transactions on Power Electronics*, vol. 38, no. 9, pp. 10579-10583, September 2023.
- [23] Fuzzy Logic Toolbox. Design and simulate fuzzy logic systems [Online]. Available: <https://www.mathworks.com/products/fuzzy-logic.html>